Chinese Chemical Letters xxx (2016) xxx–xxx

Contents lists available at ScienceDirect

Chinese Chemical Letters

journal homepage: www.elsevier.com/locate/cclet

Original article

# New π-conjugated cyanostilbene derivatives: Synthesis, characterization and aggregation-induced emission

Q1 Fang Wang [a,b], Xue Li [a,b], Sheng Wang [a,b,*], Chengpeng Li [b], Huan Dong [c], Xiang Ma [c,**], Sung-Hoon Kim [d], Derong Cao [a,**]

[a] School of Chemistry and Chemical Engineering, State Key Laboratory of Luminescent Materials and Devices, South China University of Technology, Guangzhou 510641, China
[b] Key Laboratory of Applied Chemistry and School of Chemistry and Chemical Engineering, Development Center for New Materials Engineering & Technology in Universities of Guangdong, Lingnan Normal University, Zhanjiang 524048, China
[c] Key Laboratory for Advanced Materials and Institute of Fine Chemicals, East China University of Science and Technology, Shanghai 200237, China
[d] Department of Advanced Organic Materials Science and Engineering, Kyungpook National University, Daegu 702701, Repulic of Korea

ARTICLE INFO

*Article history:*
Received 15 March 2016
Received in revised form 17 April 2016
Accepted 21 April 2016
Available online xxx

*Keywords:*
π-Conjugated cyanostilbene derivatives
1,4-Dihydropyrro[3,2-b]indole
Tetraphenylethylene
Aggregation-induced emission
Materials Studio

ABSTRACT

Two novel π-conjugated cyanostilbene derivatives, FLU-CNPH and TPE-CNPH, were designed and synthesized by introducing the strong electron donor 1, 4-dihydropyrro[3,2-b]indole and AIE electron donor tetraphenylethylene (TPE) to the (3′,5′-bis(trifluoromethyl)-biphenyl-4-yl)-acetonitrile, respectively. Both of them were fully characterized and their AIE behaviors were investigated using fluorescence spectroscopy and FE-SEM images. Their optimized structures and frontier molecular orbitals were calculated with the DFT by using Materials Studio 7.0 software to study the relationship between the structure and properties.


## 1. Introduction

Fluorescence as a detection signal can be readily recognized with good sensitivity and easy to detect. Fluorescent products can be seen everywhere in our daily life, which have made a great contribution to the various field of society. But most organic fluorescent molecules will encounter fluorescence quenching or weakening when they are in high concentrations or aggregated state, which is known as "aggregation-caused quenching" (ACQ) and hinders their wide practical applications in polymer film or solid state to a certain extent [1–4]. It is worth celebrating that in 2001 Tang group firstly discovered a new type of organic fluorescent molecules [5] showing the aggregation-induced emission (AIE) properties that the photoluminescence efficiency was greatly improved in aggregates, which could well solve the ACQ problem of conventional fluorescent molecules. This discovery provides a new direction to design organic fluorescent materials with more practical promising application [6–10].

In recent years, many researchers have developed various AIE systems [11–16]. At present, the reported AIE compounds can be mainly classified into the following categories: siloles [17], substituted ethenes [18], CN-substituted phenylene vinylenes [19], pyrans [20], biphenyl compounds [21], and polymers [22]. Accordingly, there are several proposed mechanism to be responsible for the AIE effect, restriction of intramolecular rotations (RIR) [23], twisted intermolecular charge transfer (TICT) [24], J-aggregate formation (JAF) [25], and excited-state intramolecular proton transfer (ESIPT) [26].

π-Conjugated cyanostilbene molecules are very typical AIE fluorescent materials owing to the J-type stacking and structural complanation [27–29], which have been attracted intensive research works as a platform for the design and fabrication of a variety of nano- and microstructures to use in organic optoelectronics in recent years [30–33]. Park's group reported a special class of aromatic organogelator (CN-TFMBE), which formed highly fluorescent organogels with AIE properties [31]. With some structural modification, it could self-assemble into highly

Q2 * Corresponding author at: School of Chemistry and Chemical Engineering, State Key Laboratory of Luminescent Materials and Devices, South China University of Technology, Guangzhou 510641, China.
** Corresponding authors.
*E-mail addresses:* dyesws@126.com (S. Wang), maxiang@ecust.edu.cn (X. Ma), drcao@scut.edu.cn (D. Cao).

http://dx.doi.org/10.1016/j.cclet.2016.04.020
1001-8417/

fluorescent single-crystalline organic nanowires [34]. Moreover, some aromatic organogelator had a gel-to-sol phase thermo-reversible transition with remarkable fluorescence variation that it was practically nonfluorescent in the sol phase but highly fluorescent in the gel phase [35], which realized the temperature-sensitive fluorescent molecule switch.

In this article, we designed and synthesized two new π-conjugated cyanostilbene derivatives by introducing the strong electron donor 1, 4-dihydropyrro[3,2-b]indole and typical AIE electron donor tetraphenylethylene (TPE) to the (3′,5′-bis(trifluoromethyl)-biphenyl-4-yl)-acetonitrile, respectively (FLU-CNPH and TPE-CNPH, shown in Scheme 1). Both of them were fully characterized by NMR, FTIR, and HSMS. UV–Vis absorption, fluorescence spectra and SEM images were used to study their AIE properties. Meanwhile, their optimized structures and frontier molecular orbitals were calculated using the Materials Studio software to investigate the relationship between the structure and properties.

## 2. Experimental

### 2.1. Materials and instruments

Most of chemicals were purchased from Aladdin and Aldrich. Solvents were purified by normal procedures and handled under moisture free atmosphere. The other materials were commercial products and were used without further purification. NMR spectra were recorded by using a Buker Avance □ 400 MHz spectrometer with TMS as internal standard. Melting points were determined using a Beijing Tech X-4 apparatus with a digital thermometer and are uncorrected. UV–visible absorption spectra were measured on a Shimadzu UV-2550 spectrophotometer. Fluorescence spectra were measured on an Agilent Cary Eclipse Fluorescence Spectrophotometer. Infrared spectra were measured on a Nicolet 6700 FT-IR spectrometer using KBr pellets. Mass spectra were recorded on a Shimadzu QP1000 spectrometer. FE-SEM images were acquired on a Hitachi S-4800 field emission scanning electron microscopy by dropping the sample liquid on the foil. A Canon EOS 60D digital camera was used to take photographs. The fluorescent quantum yields ($\Phi_f$) of FLU-CNPH and TPE-CNPH solutions were measured with rhodamine B in ethanol ($\Phi_f$ = 89%) as the standard [36].

### 2.2. Synthesis procedures of FLU-CNPH and TPE-CNPH

The intermediate compounds **3**, **5**–**8**, **10** were prepared by the routes outlined in Scheme S1. The detailed procedures and characterization data are deposited in supporting information.

Compound FLU-CNPH. The mixture of **8** (0.16 g, 0.4 mmol) and **3** (0.13 g, 0.4 mmol) in *tert*-butyl alcohol (10 mL) and THF (0.4 mL) was stirred at 50 C for 1 h. Tetrabutylammonium hydroxide (TBAH) (0.04 mmol, 1 mol/L in methanol) was slowly dropped into the mixture and stirred for 1 h. The red precipitate was collected by filtration and washed with methanol. Silica column purification (PE: EA = 2: 1 as eluent) was carried out to give a red powder with a yield of 57%. Mp: 194–195°C. $^1$H NMR (400 MHz, chloroform-*d*): δ 8.04 (s, 2H), 7.88 (s, 1H), 7.78 (d, 2H, *J* = 8.4 Hz), 7.67 (d, 2H, *J* = 8.4 Hz), 7.61 (d, 1H, *J* = 8.4 Hz), 7.56 (s, 1H), 7.42 (s, 1H), 7.38 (s, 1H), 7.21 (d, 1H, *J* = 8.4 Hz), 4.09 (s, 3H), 4.04–3.91 (m, 2H), 2.09–1.97 (m, 1H), 1.45–1.21 (m, 9H), 0.91 (dt, 6H, *J* = 14.1, 7.2 Hz). $^{13}$C NMR (101 MHz, chloroform-*d*): δ 144.21, 142.24, 137.42, 135.97, 135.87, 132.45, 132.12, 132.08, 128.39, 127.79, 126.89, 125.88, 124.68, 121.97, 121.40, 121.17, 119.32, 118.63, 117.04, 113.06, 112.85, 101.50, 93.64, 48.97, 39.34, 32.32, 31.95, 30.68, 29.73, 29.39, 28.59, 24.09, 23.08, 22.72, 14.16, 14.07, 10.74. FT-IR (KBr, cm$^{-1}$): 2963.55, 2926.97, 2857.88, 2210.59, 1565.62, 1496.67, 1453.33, 1415.58, 1379.13, 1277.05, 1178.46, 1142.04. HRMS (ESI): *m*/*z* 699.1678 [M + Na] $^+$.

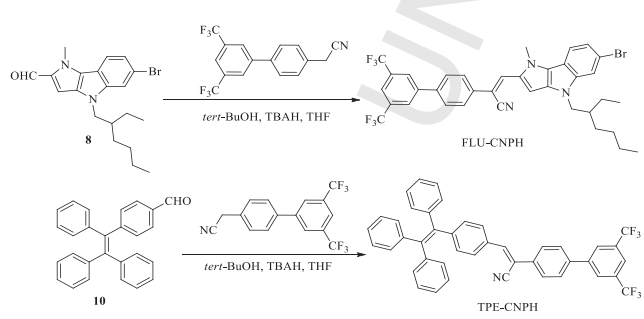


**Scheme 1.** Synthetic procedures of FLU-CNPH and TPE-CNPH.

Compound TPE-CNPH. The mixture of **10** (0.18 g, 0.5 mmol) and **3** (0.16 g, 0.5 mmol) in tert-butyl alcohol (10 mL) and THF (0.5 mL) was stirred at 50 C for 1 h. Tetrabutylammonium hydroxide (TBAH) (0.05 mmol, 1 mol/L in methanol) was slowly dropped into the mixture and stirred for 1 h. The yellow precipitate was collected by filtration and washed with methanol. Silica column purification (PE: EA = 5: 1 as eluent) was carried out to give a light yellow powder with a yield of 61%. Mp: 180–181°C. $^1$H NMR (400 MHz, chloroform-*d*): δ 8.04 (s, 2H), 7.89 (s, 1H), 7.78 (d, 2H, *J* = 8.2 Hz), 7.69 (t, 4H, *J* = 8.5 Hz), 7.50 (s, 1H), 7.14 (t, 11H, *J* = 8.5 Hz), 7.10–6.97 (m, 6H). $^{13}$C NMR (101 MHz, Chloroform-*d*): δ 146.95, 143.28, 143.13, 142.55, 142.53, 142.14, 139.94, 138.64, 135.30, 132.49, 132.16, 132.02, 131.37, 131.34, 131.29, 128.94, 127.93, 127.89, 127.85, 127.71, 127.10, 126.95, 126.78, 126.76, 126.73, 124.65, 121.94, 121.38, 117.92, 109.58. FT-IR (KBr, cm$^{-1}$): 3056.33, 3026.33, 2215.73, 1592.94, 1492.36, 1445.46, 1381.63, 1280.30, 1179.92, 1136.61, 700.63. HRMS (ESI): *m*/*z* 694.1954 [M + Na] $^+$.

## 3. Results and discussion

### 3.1. The design and synthesis of FLU-CNPH and TPE-CNPH

The synthetic routes leading to compounds FLU-CNPH and TPE-CNPH are shown in Scheme 1. The key compound **8** was prepared by a crafty route from 1-methyl-1*H*-pyrrole, which had experienced an excellent regioselectivity C–H bond activation reaction, one step direct cyclization reaction, alkylation, and formylation reaction in turn (Scheme S1 in Supporting information). Compared to the structure of carbazole, the structure of 1, 4-dihydropyrro[3,2-b]indole contains more nitrogen atoms which endow it the stronger electron donating ability. Moreover, another structure TPE as a typical AIE luminogen is also an electron donor. In our work, we tried to respectively connect the two structures to π-conjugated cyanostilbene group, which was another typical AIE luminogen with a strong electron-withdrawing cyano group, and discussed the AIE properties of the convergence structure.

### 3.2. AIE properties of FLU-CNPH and TPE-CNPH

Fig. 1 shows the UV–Vis absorption and PL spectra of FLU-CNPH and TPE-CNPH in solution. The maximum absorption peaks at 377 nm and 461 nm were mainly assigned to the absorption of the structure of 1, 4-dihydropyrro[3,2-b]indole and TPE, respectively. Their maximum emission wavelengths were both at 522 nm, but the Stokes shift of TPE-CNPH (145 nm) is much larger than that of FLU-CNPH (61 nm), which means TPE-CNPH can be selected as an ideal fluorophore. Meanwhile, TPE-CNPH is not completely non-emissive in dilute solutions but not weak fluorescence emission ($\Phi_f$ = 1.5%). This was probably because the rotation of the benzene ring directly connected to cyanostilbene group was restricted to some extent. As shown in the Fig. 2, by adding water to the solution, the luminescence intensity of TPE-CNPH was highly



Please cite this article in press as: F. Wang, et al., New π-conjugated cyanostilbene derivatives: Synthesis, characterization and aggregation-induced emission, Chin. Chem. Lett. (2016), http://dx.doi.org/10.1016/j.cclet.2016.04.020

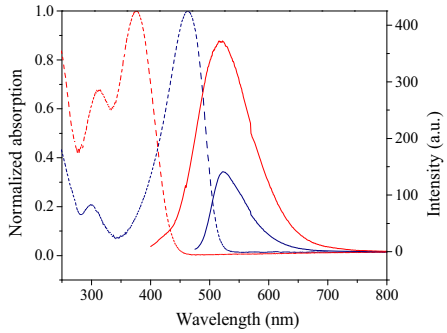


**Fig. 1.** UV–Vis absorption (dashed lines) and PL (solid lines) spectra of TPE-CNPH (red) and FLU-CNPH (blue) THF solutions (concentration: 10 mmol/L). The excitation wavelength was kept at 375 nm for TPE-CNPH and 462 nm for FLU-CNPH.

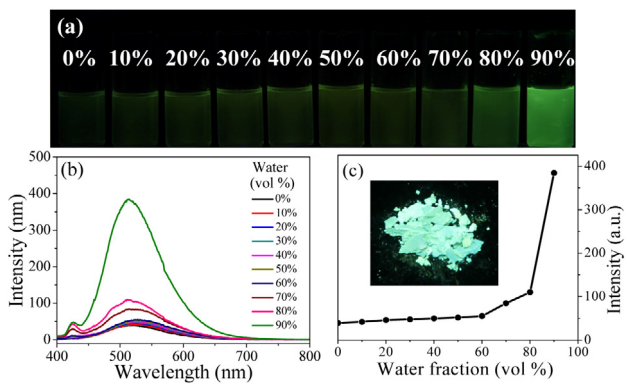


**Fig. 2.** (a) PL photos under UV (365 nm) light, (b) PL spectra of TPE-CNPH in different water-THF (v/v) mixtures, (c) The dependence of the fluorescence emission intensity on the water fraction (inset: luminescent picture of the solid powder of TPE-CNPH under 365 nm). Concentration: 20 mmol/L, excitation wavelength: 375 nm.

enhanced by 10 times with water fraction 90 vol% ($\Phi_f$ = 16%). Because TPE-CNPH was not so solvable in water, the molecules aggregated in the mixture, which activated the RIR process and the PL intensity was enhanced.

Different from the AIE properties of TPE-CNPH, a red-shift of fluorescence emission was obviously observed in FLU-CNPH solutions with water volume fraction increasing, accompanied by the formation of different aggregates (Fig. 3). As shown in Fig. 3a, only very weak yellowish green fluorescence ($\Phi_f$ = 0.09% for 0 vol%, 0.12% for 50 vol%) was observed in the THF-$H_2O$ mixtures of FLU-CNPH when the water fraction was no higher than 50 vol%. However, the fluorescence intensity was swiftly enhanced with a water fraction of 60 vol% ($\Phi_f$ = 2.4%). Meanwhile, the fluorescent colors turned to yellow-orange with many strong fluorescent granular precipitates formation in the mixture. But the fluorescence intensity decreased when the water fraction was increased to 70 vol% ($\Phi_f$ = 0.6%) or more, the mixtures all became homogeneous suspensions with no precipitates and the fluorescent colors finally turned red with a water fraction of 90 vol% ($\Phi_f$ = 0.6%).

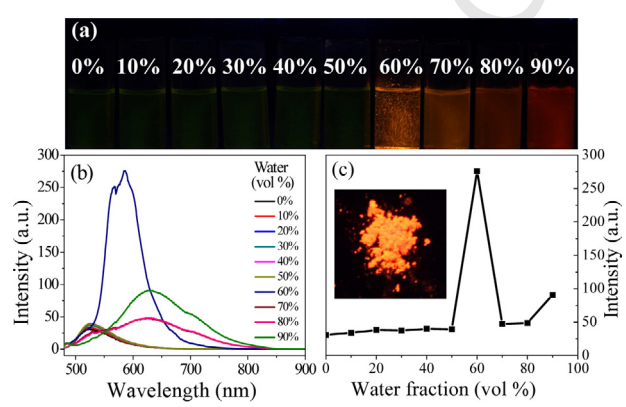


**Fig. 3.** (a) PL photos under UV (365 nm) light, (b) PL spectra of FLU-CNPH in different water-THF (v/v) mixtures, (c) The dependence of the fluorescence emission intensity on the water fraction (inset: luminescent picture of the solid powder of FLU-CNPH under 365 nm). Concentration: 20 mmol/L, excitation wavelength: 462 nm.

To better understand the AIE properties of TPE-CNPH and FLU-CNPH, FE-SEM images of their aggregates were studied (Fig. 4). Surprisingly, the microstructure like morning glory of FLU-CNPH was obtained by 60 vol% fractions of water addition, a flower or a bunch of flowers was dispersed in the THF-$H_2O$ mixture (Fig. 4a). With a water fraction of 90 vol%, more aggregates were obtained because of its poorer solubility. The regular "flower" shape disappeared and was replaced by FLU-CNPH nanoparticles, which were similar to the shape of small round cakes and stuck together with each other (Fig. 4b). The strong π–π interactions between molecules would prompt the formation of excimers and this detrimental species led to the observed fluorescence quenching of FLU-CNPH in 90 vol% mixture. FE-SEM pictures in Fig. 4c show that TPE-CNPH nanoscale sticks obtained with a water fraction of 90 vol% were cross or parallel to stick together with each other. Compared to the nanoparticles in Fig. 4b, the nanosticks have more regular geometric structure and the TPE-CNPH molecular packing are relatively more loose leading to the weaker π–π interactions, so the RIR process is most responsible for the AIE behavior of TPE-CNPH.

### 3.3. Theoretical calculations of geometrical and electronic properties

In order to understand more about the relationship between the molecular structure and performance of FLU-CNPH and TPE-CNPH, their optimized structures and electronic distribution of HOMO and LUMO energy levels were obtained by molecular orbital calculations with the DFT by using Materials Studio 7.0 software on GGA/BLYP levels, as shown in Fig. 5. The four benzene rings on double bond of TPE-CNPH were all in different plane but the benzene ring directly connected to the cyanostilbene structure was on the plane of cyanostilbene with a small dihedral angle, which explained the weak fluorescence of TPE-CNPH in THF solution. Similarly, the 1, 4-dihydropyrro[3,2-b]indole and cyanostilbene structure can be considered to be in the same plane but the long branched alkanes was approximatively perpendicular to the plane. On this basis, we could explain the different aggregation formation which caused the unique AIE properties of FLU-CNPH. With the low

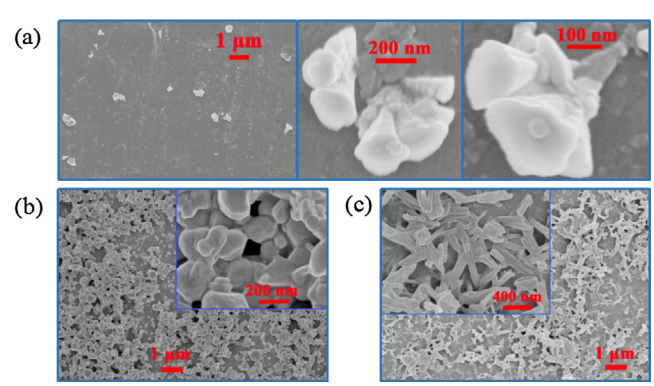


**Fig. 4.** FE-SEM images of FLU-CNPH (a) in $H_2O$-THF (v: $v$ = 6:4, 2.0 × $10^{-5}$ mol/L) mixture, (b) in $H_2O$-THF (v:$v$ = 9:1, 2.0 × $10^{-5}$ mol/L) mixture, (c) FE-SEM images of TPE-CNPH in $H_2O$-THF (v:$v$ = 9:1, 2.0 × $10^{-5}$ mol/L) mixture.



Please cite this article in press as: F. Wang, et al., New π-conjugated cyanostilbene derivatives: Synthesis, characterization and aggregation-induced emission, Chin. Chem. Lett. (2016), http://dx.doi.org/10.1016/j.cclet.2016.04.020

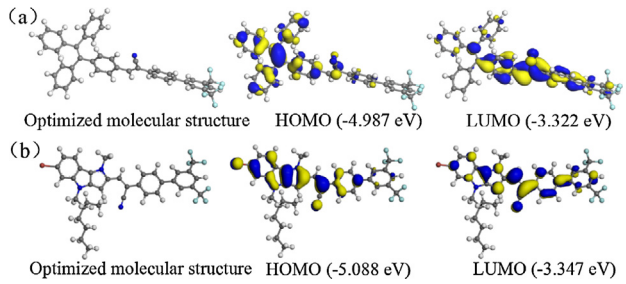


**Fig. 5.** Optimized structures and frontier molecular orbitals of (a) TPE-CNPH and (b) FLU-CNPH.

water fraction 60 vol% the molecules of FLU-CNPH would slowly assemble in an ordered fashion, like J-type aggregates, which was more emissive. While in the water fraction above 60 vol%, the more tightly packed structure was obtained in a random way, which would make it less emissive owing to the molecular planarity and strong π–π stacking interactions. But the flexibility of long branched alkanes could reduce this effect to a certain extent so that the fluorescence intensity in the water fraction above 60 vol% had decreased but still stronger than that of the 0 vol% mixture, accompanied by the red shift of fluorescence spectra.

The HOMO of TPE-CNPH was mainly localized over the TPE moiety and its LUMO was located on the cyanostilbene group. As shown in Fig. 5, the HOMO and LUMO energy levels were well separated in TPE-CNPH molecule, which was in favor of a facile charge migration. But, for FLU-CNPH, the LUMO and HOMO were localized over the whole molecule which suggested a poor charge transfer propensity.

## 4. Conclusion

In conclusion, we designed and synthesized two novel π-conjugated cyanostilbene derivatives, FLU-CNPH and TPE-CNPH. Both of them were AIE active that had been proven by the fluorescence spectroscopy and morphology studies in different solvent-water mixtures. FLU-CNPH would experience two different aggregation formations with the water fraction increasing, nanoparticles like morning glory flower and nanoparticles like small round cakes. When the water fraction was above 60 vol%, the fluorescence intensity was reduced because of its rigid structure in consistent with the red shift of the fluorescence spectra. The RIR process played an important role in the AIE behavior of TPE-CNPH. Their HOMO and LUMO were calculated using Materials Studio 7.0 software, indicating a good charge transfer propensity of TPE-CNPH.

## Acknowledgment

This work was financially supported by NSFC (Nos. 21372194, 21476075 and 21272072) and the Guangdong Yangfan Talent Plan (2013). Chengpeng Li also acknowledge the Research Funds of Lingnan Normal University (No. QL1402).

## Appendix A. Supplementary data

Supplementary data associated with this article can be found, in the online version, at http://dx.doi.org/10.1016/j.cclet.2016.04.020.

## References

[1] J. Mei, N.L.C. Leung, R.T.K. Kwok, J.W.Y. Lam, B.Z. Tang, Aggregation-induced emission: together we shine, united we soar, Chem. Rev. 115 (2015) 11718–11940.
[2] Y. Hong, J.W.Y. Lamab, B.Z. Tang, Aggregation-induced emission, Chem. Soc. Rev. 40 (2011) 5361–5388.
[3] R. Hu, N.L. Leung, B.Z. Tang, AIE macromolecules: syntheses, structures and functionalities, Chem. Soc. Rev. 43 (2014) 4494–4562.
[4] J. Mei, Y. Hong, J.W. Lam, et al., Aggregation-induced emission: the whole is more brilliant than the parts, Adv. Mater. 26 (2014) 5429–5479.
[5] J. Luo, Z. Xie, J.W.Y. Lam, et al., Aggregation-induced emission of 1-methyl-1,2,3,4,5-pentaphenylsilole, Chem. Commun. (2001) 1740–1741.
[6] J. Liang, B.Z. Tang, B. Liu, Specific light-up bioprobes based on AIEgen conjugates, Chem. Soc. Rev. 44 (2015) 2798–2811.
[7] A. Ozawa, A. Shimizu, R. Nishiyabu, Y. Kubo, Thermo-responsive white-light emission based on tetraphenylethylene- and rhodamine B-containing boronate nanoparticles, Chem. Commun. 51 (2015) 118–121.
[8] X. Zhang, X. Zhang, B. Yang, Y. Zhang, Y. Wei, A new class of red fluorescent organic nanoparticles: noncovalent fabrication and cell imaging applications, ACS Appl. Mater. Interfaces 6 (2014) 3600–3606.
[9] J. Geng, Z. Zhu, W. Qin, et al., Near-infrared fluorescence amplified organic nanoparticles with aggregation-induced emission characteristics for *in vivo* imaging, Nanoscale 6 (2014) 939–945.
[10] H. Lu, B. Xu, Y. Dong, et al., Novel fluorescent pH sensors and a biological probe based on anthracene derivatives with aggregation-induced emission characteristics, Langmuir 26 (2010) 6838–6844.
[11] H. Li, X. Zhang, Z. Chi, et al., New thermally stable piezofluorochromic aggregation-induced emission compounds, Org. Lett. 13 (2011) 556–559.
[12] Y.L. Zhang, J. Li, B.Z. Tang, K.S. Wong, Aggregation enhancement on two-photon optical properties of AIE-active D-TPE-A molecules, J. Phys. Chem. C 118 (2014) 26981–26986.
[13] X. Zhang, X. Zhang, L. Tao, et al., Aggregation induced emission-based fluorescent nanoparticles: fabrication methodologies and biomedical applications, J. Mater. Chem. B 2 (2014) 4398–4414.
[14] A. Kathiravan, K. Sundaravel, M. Jaccob, et al., Pyrene Schiff base: photophysics, aggregation induced emission and antimicrobial properties, J. Phys. Chem. B 118 (2014) 13573–13581.
[15] Y. Dong, J.W. Lam, A. Qin, et al., Aggregation-induced and crystallization-enhanced emissions of 1,2-diphenyl-3,4-bis(diphenylmethylene)-1-cyclobutene, Chem. Commun. (2007) 3255–3257.
[16] P. Zhang, H. Wang, H. Liu, M. Li, Fluorescence-enhanced organogels and mesomorphic superstructure based on hydrazine derivatives, Langmuir 26 (2010) 10183–10190.
[17] J. Liu, Y. Zhong, J.W.Y. Lam, et al., Hyperbranched conjugated polysiloles: synthesis, structure, aggregation-enhanced emission, multicolor fluorescent photopatterning, and superamplified detection of explosive, Macromolecules 43 (2010) 4921–4936.
[18] Z. Zhao, J.W.Y. Lam, B.Z. Tang, Tetraphenylethene: a versatile AIE building block for the construction of efficient luminescent materials for organic light-emitting diodes, J. Mater. Chem. 22 (2012) 23726.
[19] B.K. An, S.K. Kwon, S.D. Jung, S.Y. Park, Enhanced emission and its switching in fluorescent organic nanoparticles, J. Am. Chem. Soc. 124 (2002) 14410–14415.
[20] G. Kwak, S. Wang, M.S. Choi, et al., 2D-π-A type pyran-based dye derivatives: photophysical properties related to intramolecular charge transfer and their electroluminescence application, Dyes Pigments 78 (2008) 25–33.
[21] H. Tong, Y. Dong, M. Haussler, et al., Tunable aggregation-induced emission of diphenyldibenzofulvenes, Chem. Commun. (2006) 1133–1135.
[22] H. Zhou, J. Li, M. Chua, et al., Poly(acrylate) with a tetraphenylethene pendant with aggregation-induced emission (AIE) characteristics: highly stable AIE-active polymer nanoparticles for effective detection of nitro compounds, Polym. Chem. 5 (2014) 5628–5637.
[23] Q. Zeng, Z. Li, Y. Dong, et al., Fluorescence enhancements of benzene-cored luminophors by restricted intramolecular rotations: AIE and AIEE effects, Chem. Commun. (2007) 70–72.
[24] R. Hu, E. Lager, A.L. Aguilar-Aguilar, et al., Twisted intramolecular charge transfer and aggregation-induced emission of BODIPY derivatives, J. Phys. Chem. C 113 (2009) 15845–15853.
[25] B.K. An, J. Gierschner, S.Y. Park, π-Conjugated cyanostilbene derivatives: a unique self-assembly motif for molecular nanostructures with enhanced emission and transport, Acc. Chem. Res. 45 (2012) 544–554.
[26] Z. Song, R.T. Kwok, E. Zhao, et al., A ratiometric fluorescent probe based on ESIPT and AIE processes for alkaline phosphatase activity assay and visualization in living cells, ACS Appl. Mater. Interfaces 6 (2014) 17245–17254.
[27] S.K. Park, J.H. Kim, S.J. Yoon, et al., High-performance n-type organic transistor with a solution-processed and exfoliation-transferred two-dimensional crystalline layered film, Chem. Mater. 24 (2012) 3263–3268.
[28] Y. Yu, Q. Shi, Y. Li, et al., Solid supramolecular architecture of a perylene diimide derivative for fluorescent enhancement chemistry, Chem. Asian J. 7 (2012) 2904–2911.
[29] Y. Li, T. Liu, H. Liu, M.Z. Tian, Y. Li, Self-assembly of intramolecular charge-transfer compounds into functional molecular systems, Acc. Chem. Res. 47 (2014) 1186–1198.
[30] C.K. Lim, S. Kim, I.C. Kwon, C.H. Ahn, S.Y. Park, Dye-condensed biopolymeric hybrids: chromophoric aggregation and self-assembly toward fluorescent bionanoparticles for near infrared bioimaging, Chem. Mater. 21 (2009) 5819–5825.
[31] J.W. Chung, Y. You, H.S. Huh, et al., Shear- and UV-induced fluorescence switching in stilbenic π-dimer crystals powered by reversible [2 + 2] cycloaddition, J. Am. Chem. Soc. 131 (2009) 8163–8172.
[32] H. Li, D.H. Qu, Recent advances in new-type molecular switches, Sci. China Chem. 58 (2015) 916–921.

[33] T.T. Cao, X.Y. Yao, J. Zhang, Q.C. Wang, X. Ma, A cucurbit[8]uril recognized rigid supramolecular polymer with photo-stimulated responsiveness, Chin. Chem. Lett. 26 (2015) 867–871.
[34] J.W. Chung, H. Yang, B. Singh, et al., Single-crystalline organic nanowires with large mobility and strong fluorescence emission: a conductive-AFM and space-charge-limited-current study, J. Mater. Chem. 19 (2009) 5920–5925.
[35] J.W. Chung, B.K. An, S.Y. Park, A thermoreversible and proton-induced gel-sol phase transition with remarkable fluorescence variation, Chem. Mater. 20 (2008) 6750–6755.
[36] X. Yang, Z.T. Pan, Y. Ma, Rhodamine B as standard substance to measure the fluorescence-quantum yield of dichlorofluorescein, J. Anal. Sci. 19 (2003) 588–589.



Please cite this article in press as: F. Wang, et al., New π-conjugated cyanostilbene derivatives: Synthesis, characterization and aggregation-induced emission, Chin. Chem. Lett. (2016), http://dx.doi.org/10.1016/j.cclet.2016.04.020